ISIJ International, Vol. 31 (1991), No. 8, pp. 882–889

Cryogenic Mechanical Properties of Ti–6Al–4V Alloys with Three Levels of Oxygen Content

Kotobu NAGAI, Tetsumi YURI, Toshio OGATA, Osamu UMEZAWA, Keisuke ISHIKAWA, Takashi NISHIMURA,[1] Takao MIZOGUCHI[2] and Yoshimasa ITO[3]

Tsukuba Laboratories, National Research Institute for Metals, Sengen, Tsukuba, Ibaraki-ken, 305 Japan. 1) Titanium Metals Technology Control Department, Kobe Steel, Ltd., Niihama, Arai-cho, Takasago, Hyogo-ken, 676 Japan. 2) Mechanical Engineering Research Laboratory, Kobe Steel, Ltd., Takatsukadai, Nishi-ku, Kobe, Hyogo-ken, 673-02 Japan. 3) Materials Research Laboratory, Kobe Steel, Ltd., Wakinohama-cho, Chuo-ku, Kobe, Hyogo-ken, 651 Japan.

(Received on February 14, 1991; accepted in final form on April 26, 1991)

Tensile, fracture toughness, and high cycle fatigue tests were done at 293, 77, and 4 K for Ti–6Al–4V alloys with three levels of oxygen content. The alloys were investigated both in as-forged condition and in the rolled condition. Rolling did not necessarily make α grains finer, but changed the shape from plate-like to globular. Strengths depended mainly on the oxygen content; the lower content produced lower strengths. The alloy with lowest oxygen content showed the best ductility at 4 K. The fracture toughness at cryogenic temperature was also enhanced by the reduction of oxygen. In the lowest oxygen alloy, no drop in the fracture toughness was observed between 293 and 4 K. Fatigue properties were influenced by the forming process. The rolled materials had higher fatigue strength than the forged materials. The difference was accentuated at 4 K. This is believed to be due to the difference in the morphology of α grains. The lowest oxygen alloy showed the highest fatigue strength at 4 K.

KEY WORDS: titanium alloy; Ti-6Al-4V alloy; yield strength; elongation; fracture toughness; high cycle fatigue; cryogenic temperature; microstructure; processing; oxygen content.

1. Introduction

Recent R & D projects based on superconductivity and cryogenics have a wide range of engineering applications like magnetic levitation car, electromagnetic thruster (ship), and superconducting generator, *etc.* For cryogenic structural materials, a high fracture toughness as well as a high yield strength has been essentially required.[1] In addition, a good fatigue strength is also needed for the new technologies,[2] since the machines experiences stop-run load cycles and they often have "moving" components. And further some other properties are potentially demanded for better heat insulation and more sound operation under high magnetic field (static or alternate).

Titanium (Ti) alloy has many advantages for the cryogenic applications. Its low specific strength, strength-to-gravity ratio, and high yield strength are very favorable for high efficiency of the "moving" machines. And further, the alloy is more blessed with the low thermal conductivity, the extremely low magnetic permeability and the high electric resistivity,[3] compared with austenitic stainless steels. These should be more appreciated as the merits of Ti alloy for cryogenic structural use.

Some of the present authors previously reported the tensile properties, fracture toughness, and high cycle fatigue properties of a Ti–5Al–2.5Sn ELI (Extra-Low-Interstitials) alloy.[4] The reduction of oxygen content yielded the high fracture toughness at 4 K. Accordingly the Ti–5Al–2.5Sn ELI alloy showed an excellent combination of yield strength and fracture toughness at 4 K and an increased fatigue strength at lower temperature.

Ti–6Al–4V alloy is one of the most popular Ti alloys and used in varieties of applications. The alloy has a higher yield strength than the Ti–5Al–2.5Sn alloy. However, few were studied on the cryogenic mechanical properties.[5] Therefore, the basic objectives of the present study were to determine the cryogenic mechanical properties of the Ti–6Al–4V alloy in tensile, fracture toughness, and fatigue tests.

It was reported the low temperature fracture toughness was fairy low in the Ti–6Al–4V alloy.[6] The room temperature fracture toughness alloy depends on metallurgical factors like purity and microstructure.[7,8] But how the low temperature toughness can be controlled has yet to be made clear. Hence in the present study, the effects of the purity on the cryogenic mechanical properties of the Ti–6Al–4V alloy were mainly focussed and, in addition, the effect of manufacturing process was also studied.

Table 1. Chemical compositions of Ti–6Al–4V alloys tested in the present study in mass%.

Alloy	Al	V	Fe	O	N	H	C
Normal	6.34	4.23	0.199	0.135	0.0071	0.0053	0.011
ELI	6.23	4.25	0.200	0.104	0.0035	0.0032	0.011
SpELI	5.97	4.12	0.028	0.054	0.0019	0.0055	0.024

Table 2. Process of forging, rolling, and heat treatment for each alloy.

Alloy	Forging	Rolling	Heat treatment
Normal	$\alpha+\beta$ forging (75×85) $\rightarrow\alpha+\beta$ forging (70×70)	$\alpha+\beta$ rolling (28ϕ)	973 K, 7.2 ks Air cooled
ELI	$\alpha+\beta$ forging (115×120) $\rightarrow\alpha+\beta$ forging (70×70)		
SpELI	β forging (170ϕ) $\rightarrow\alpha+\beta$ forging (70×70)		

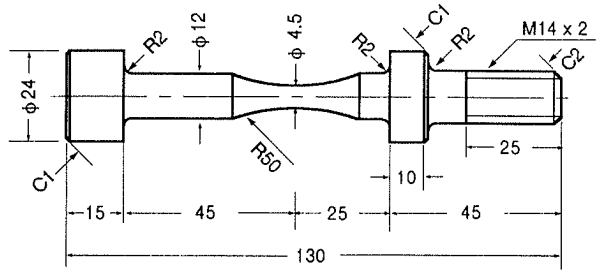

Fig. 1. Specimen geometry of fatigue test piece. The minimum waist of some specimens was 6 mm.

2. Experimental Procedure

2.1. Test Materials

Three Ti–6Al–4V alloys with different impurity levels were melted; namely a normal-grade one (Normal), an extra-low-interstitial grade one (ELI),[9] and an extremely-low-interstitial grade one (Special ELI, abbreviated as SpELI here). They had different oxygen contents and the nominal oxygen content was 0.15, 0.10 and 0.05 mass%. In the SpELI alloy, iron was intentionally unadded expecting a better toughness,[6] although 0.2% iron was conventionally added in other two alloys. The chemical compositions are listed in **Table 1**.

Each ingot was forged finally in $\alpha+\beta$ region (1 173 K) and it is called "forged material" in the present paper. And then a part of the forged material for each alloy was rolled also in $\alpha+\beta$ region (1 173 K); it is called "rolled material". All the materials were finally heat-treated for 7.2 ks at 973 K and air-cooled. Some details of the processing history are shown in **Table 2**.

2.2. Tensile Test

Cylindrical test pieces were cut parallel to the longitudinal direction (L-direction) for both the forged and the rolled materials. The gage geometry was 3.5 mm in diameter and 20 mm in length. Tests were done at a strain rate of $8.33\times10^{-4}\,\mathrm{sec}^{-1}$ using a screw-driven type tester. The test temperatures were 293, 77, and 4 K. Yield strength (principally 0.2% offset stress), tensile strength, elongation (fracture strain), and reduction of area were determined by duplicate test.

2.3. Fracture Toughness Test

Compact tension (CT) specimens with a thickness of 25 mm were machined so that the load axis was parallel to the longitudinal direction of the forged bars and the crack plane parallel to the short transverse. The rolled material did not have the size enough for the CT specimen. The fracture toughness, K_{IC}(J), was determined by unloading compliance method[10] in accordance with ASTM E813-81. The fatigue precrack with a length of 60% specimen thickness was introduced at room temperature. A servo-hydraulic test machine was used and the time from zero load to maximum load was between 5 and 10 min.

2.4. High Cycle Fatigue Test

Hourglass type unnotched specimens drawn in **Fig. 1** were machined in the L-direction for both the forged and the rolled materials. S–N curves at 293, 77, and 4 K were determined using the cryogenic fatigue test machine.[11] In obtaining the S–N curves, the estimation of a million cycles fatigue strength (MFS) was intended. The test machine was servo-hydraulic and its dynamic capacity was $\pm$50 kN. Load control test was done in a sinusoidal wave with a minimum-to-maximum load ratio, $R=0.01$ at 4 Hz at 4 K and at 10–20 Hz at 77 and 293 K.

3. Results and Discussion

3.1. Microstructure

In the rolled material, the reduction ratio in section areas was 7.9 times more than in the forged material. Therefore, a finer and more homogeneous microstructure was expected for the rolled material. **Figure 2** represents the SEM photographs of miscrostructures for the materials tested here. The forged materials have lamellar microstructure principally composed of elongated or plate-like primary α grain and β (or transformed β) platelet. The formation of "colony", namely the region in which α plates are aligned, is seen especially in ELI and SpELI alloys. The mean width of α grain was 5.0, 4.0, and 1.9 μm in Normal, ELI, and SpELI, respectively. In the rolled materials, the α grain and the β particle become globular. The mean diameter of α gain was 4.0, 4.0, and 2.8 μm in Normal, ELI, and SpELI, respectively.

Rolling process did not always make α grains fine. The Normal and the ELI alloys had almost the same α grain size. The SpELI alloy had the finest microstructure, but the reason is not made clear.

3.2. Tensile Properties

Tensile properties are listed in **Table 3**. The lower the oxygen content, the lower the yield strength. The rolled

Table 3. Tensile properties and fracture toughness of Ti–6Al–4V alloys.

Alloy	Processing	T (K)	YS (MPa)	TS (MPa)	ELN (%)	RA (%)	K_{IC}(J) (MPa$\sqrt{m}$)
Normal	Forged	293	971	1 007	13.8	46.1	59.9
		77	1 482	1 573	12.1	35.7	35.1
		4	1 753	1 764	2.2	27.5	18.3
	Rolled	293	1 017	1 053	14.6	41.3	—
		77	1 590	1 634	10.1	26.1	—
		4	1 865	1 865	0.1	25.1	—
ELI	Forged	293	908	953	11.7	41.5	57.5
		77	1 447	1 502	13.8	22.0	42.9
		4	1 705	1 716	2.1	27.2	44.9
	Rolled	293	961	1 011	14.1	38.9	—
		77	1 527	1 576	13.5	27.3	—
		4	1 819	1 819	0.2	27.4	—
SpELI	Forged	293	856	891	12.9	40.8	61.8
		77	1 375	1 427	12.2	38.3	59.2
		4	1 599	1 599	5.3	33.4	62.7
	Rolled	293	887	915	14.2	52.1	—
		77	1 402	1 438	12.2	37.9	—
		4	1 674	1 674	2.3	37.3	—

T: Test temperature, YS; Yield strength, TS: Tensile strength, ELN: Elongation, RA: Reduction of area, K_{IC}(J): Fracture toughness, —: Not determined due to lack of thickness.

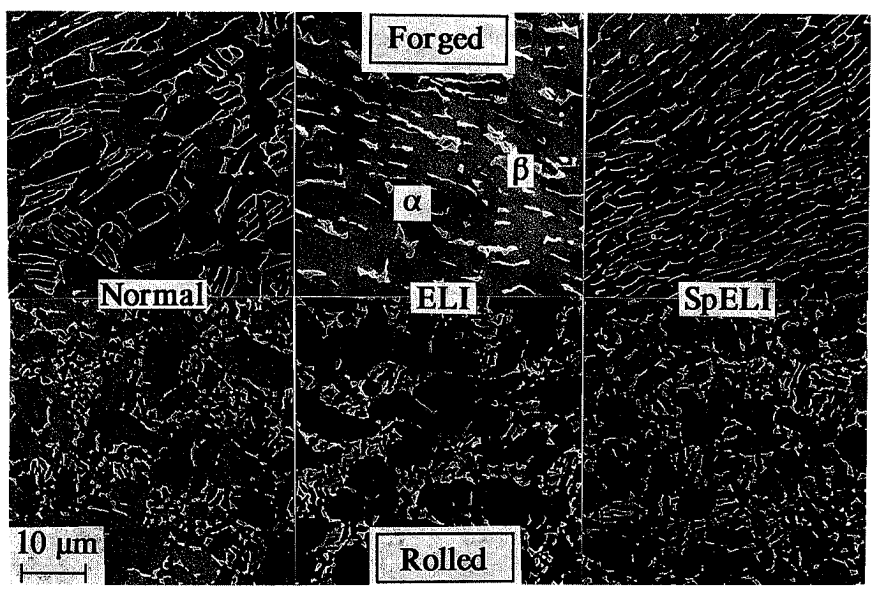

Fig. 2. SEM photographs of microstructure. The print planes are on the transverse section to the longitudinal direction of bars.

material had higher yield strength than the forged one. Yield strength and tensile strength increased with a decrease in temperature as shown in **Fig. 3**. The room temperature yield strength of Ti–6Al–4V alloy varies by the chemical composition and the heat treatment, and it can be explained in terms of change in volume fraction of α and α', their hardness and α grain size.[12] In the present study, however, the yield strength did not show a Hall-Petch type dependence on α grain size (**Fig. 4(a)**) except for the Normal alloy. The grain size dependence might appear for the forged ELI and SpELI alloys if the colony size is taken in place of α grain size. However, the yield strength of the present alloys depended obviously on the oxygen content as seen in **Fig. 4(b)**.

The ductility at 293 and 77 K did not clearly depend on the oxygen content and the processing. At 4 K, the SpELI alloy had a higher ductility than others (see Fig. 7(a)). The elongation did not largely change from 293 to 77 K, however, it dropped significantly at 4 K. On the other hand, the reduction of area revealed no drop at 4 K although it showed a slight decrease from 293 to 77 K. In **Fig. 5**, the diameter changes of the gage length at 293, 77 and 4 K are described for the fractured tensile test pieces of the forged SpELI alloy. This demonstrates that the deformation at 4 K was concentrated into a necked region and other part did not deform plastically.

At other temperatures, some amount of plastic deformation covered the gage length. In the stress–strain curves at 4 K, a characteristic phenomenon, so-called "serration", was usually observed. The serration, discontinuous flow or plastic instability, at cryogenic temperature is inherently localized or heterogeneous plastic deformation due to an extreme lowness of heat capacity and heat diffusivity in metals at cryogenic temperature.[13] The frequency and magnitude of discontinuity depend on materials, strain rate, and so on. Once a serration accompanying a small necking occurs, the flow strength (load) in undeformed region competes with that in the necked region. With an adequate strain hardening, the flow strength in the necked region is higher than that in the undeformed region. However when the strain hardening is small, the next serration (necking) occurs in the already necked region one after another. In that case, no plastic deformation takes place in the unnecked region. Thus it can be concluded that, in the Ti–6Al–4V alloy, the deformation localization in a small part of the gage length is ascribed to an apparent drop in elongation at 4 K, since the elongation is determined by the ratio of the extension to the initial value of whole gage length.

3.3. Fracture Toughness

Figure 6 shows the temperature dependence of the fracture toughness, K_{IC}(J) in the forged alloys. In the Normal alloy, the decrease in fracture toughness from 293 K to 4 K is 40 MPa$\sqrt{m}$, however in the SpELI alloy,

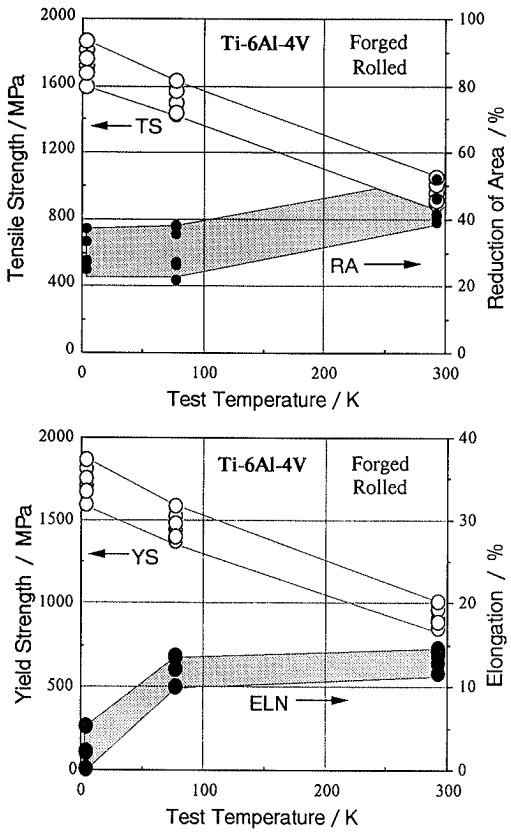

Fig. 3. Temperature dependence of tensile properties.

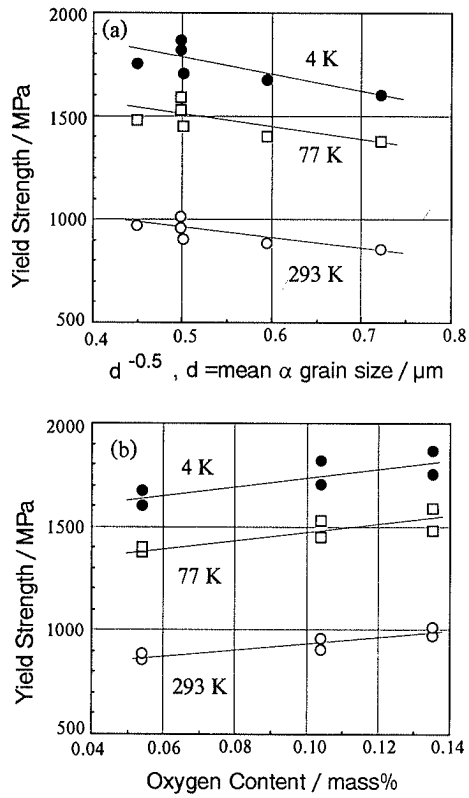

Fig. 4. Relationship between yield strength and (a) mean α grain size and (b) oxygen content.

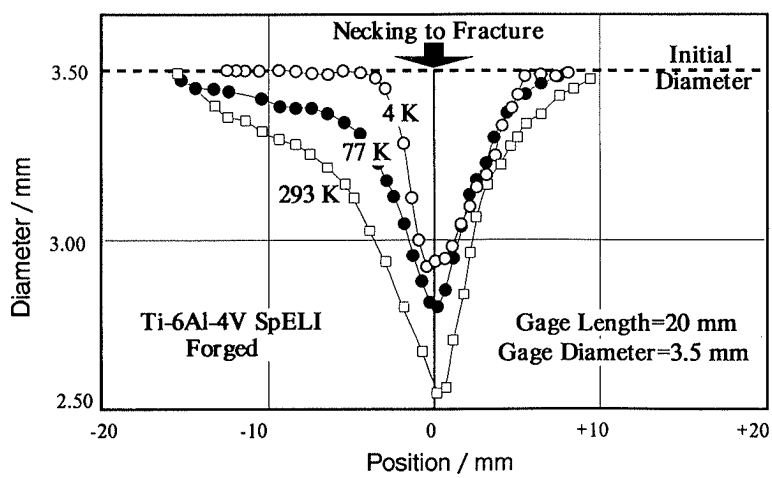

Fig. 5. Gage diameter distribution of the fractured tensile test pieces of forged Ti–6Al–4V SpELI alloy.

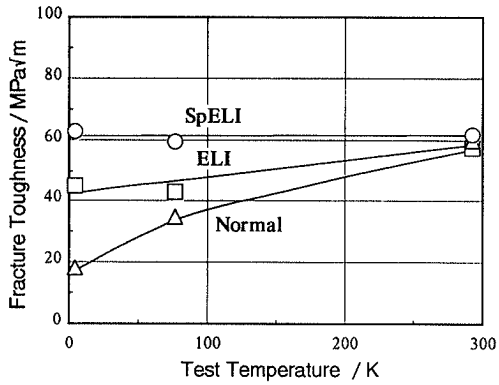

Fig. 6. Temperature dependence of fracture toughness, K_{IC}(J).

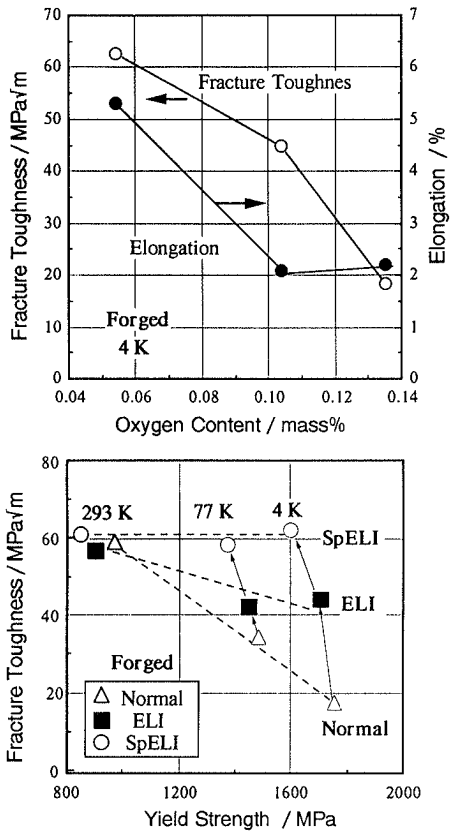

Fig. 7. Interrelationship between the fracture toughness of forged materials and other factors: (a) oxygen content and (b) yield strength. Elongation is also plotted in (a).

on the contrary, no drop is seen.

Compared with the Normal alloy, the fracture toughness of the SpELI alloy is only 2 MPa$\sqrt{m}$ (5% improvement) higher at 293 K but 45 MPa$\sqrt{m}$ (240% improvement) higher at 4 K. Thus the reduction of oxygen content brought about a remarkable improvement in the low temperature toughness of the Ti–6Al–4V alloy as demonstrated in **Fig. 7(a)**. The elimination of iron in the SpELI alloy is believed to assist this improvement.[6] The fracture toughness generally decreases inversely to an increase in the yield strength.[3] **Figure 7(b)** shows the interrelationship between yield strength and fracture toughness for all the temperature data of three alloys. Either when the temperature varies in each alloy except the SpELI alloy or when the impurity varies in a given temperature except 293 K, the fracture toughness decreases almost linearly with an increase in yield strength. In various types of Ti alloy, the slope of linear correlation is about -0.2 at 4 K,[3] which is also fitting for the present result. In this sense, it might be said that the fracture toughness at 4 K was improved by softening due to the reduction of oxygen content. But the same explanation cannot be made for the 293 K data. One evident conclusion is that the reduction of oxygen content depresses the deterioration of fracture toughness at low temperature. This is quite analogous to the effect of carbon in ferritic iron on the low temperature brittleness. However the fracture surfaces of all the materials were covered principally with small equiaxed dimples (several μm in diameter) at every temperature and no brittle failure occurred. Only Tobler reported an abrupt transition of fracture toughness at cryogenic temperatures in a Ti–6Al–4V ELI alloy[5] and he explained it by a ductile-to-brittle transition without any evidence of brittle fracture. However, the fracture mode at cryogenic temperatures is not brittle and the abrupt transition is not a common phenomenon in Ti–6Al–4V alloys[14] including the present alloys.

One evidence which may explain the effect of oxygen content on the fracture toughness is the increased crack propagation resistance with a decrease in oxygen content even at 293 K. The increment in J-integral per crack extension, $\Delta J/\Delta a$, estimated from R-curves in fracture toughness tests was 3.4, 10.3, and 17.9 MN/m^2 for the Normal, ELI, and SpELI at 293 K, respectively. The similar trend was also observed at 77 and 4 K. Horiya *et al.* explain the mechanism that an increase in crack extension resistance brings about an improvement in measured fracture toughness.[15] However, how the crack extension resistance is enhanced by the reduction of oxygen content should be studied more in details.

The present result showed the reduction of oxygen content down to as low as 0.05 mass% brought about the excellent fracture toughness at 4 K as well as at RT. Less oxygen content is considered to be very hard to produce practically. If higher fracture toughness is required, how to increase the room temperature fracture toughness must be first considered. Heat treatments, *i.e.* optimized β treatments, yielded a high fracture toughness at 4 K of the same level at room temperature in Ti–6Al–4V alloys,[14] however the improved fracture toughness did not depend much on the oxygen content. In Ti alloys, for example, the Charpy absorbed energy of over 100 J was introduced only when large equiaxed dimples (several 10 μm in diameter) were major in the fracture surfaces.[3] Hence, changing the fracture mode into more ductile one, although it has yet to be elucidated, may be a possible way to enhance the fracture toughness more.

3.4. High Cycle Fatigue Property

All the S–N curves obtained in the present study are described in **Figs. 8** to **10**. In these materials, two kinds of fatigue crack initiation site were observed. One was conventionally at the specimen surface, and the other was in the specimen interior. SEM photographs of the

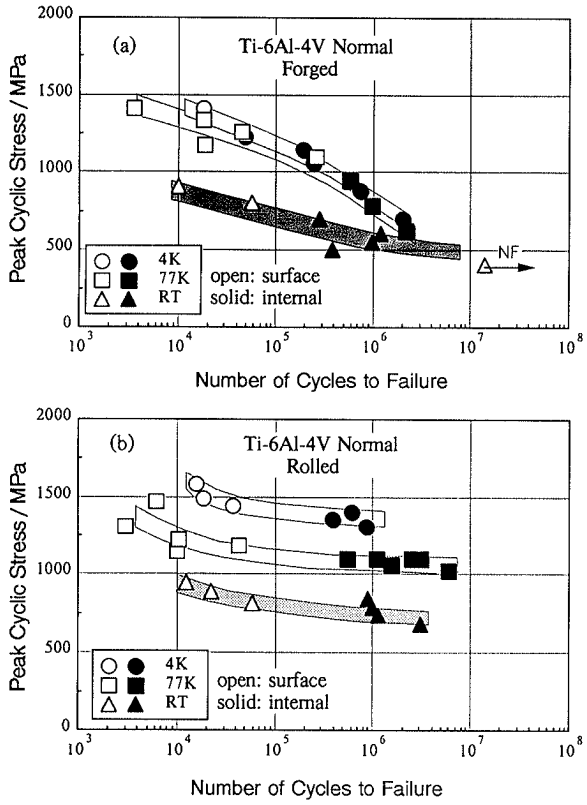

Fig. 8. S–N curves of Ti–6Al–4V normal alloys: (a) forged and (b) rolled.

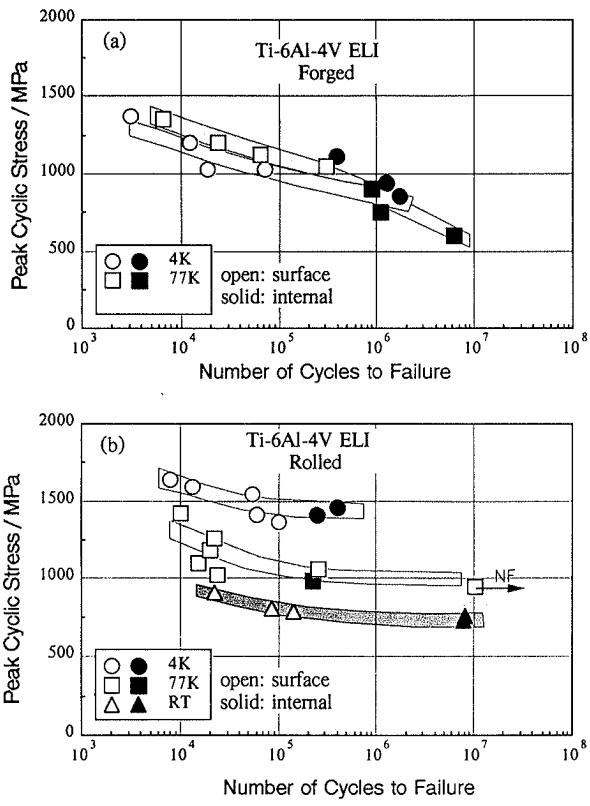

Fig. 9. S–N curves of Ti–6Al–4V ELI alloys: (a) forged and (b) rolled.

latter cases are presented in **Fig. 11**. In Figs. 8 to 10, therefore, the crack initiation sites are classified into "Surface" or "Internal". The internal fatigue crack initiation in the present alloys is discussed in details

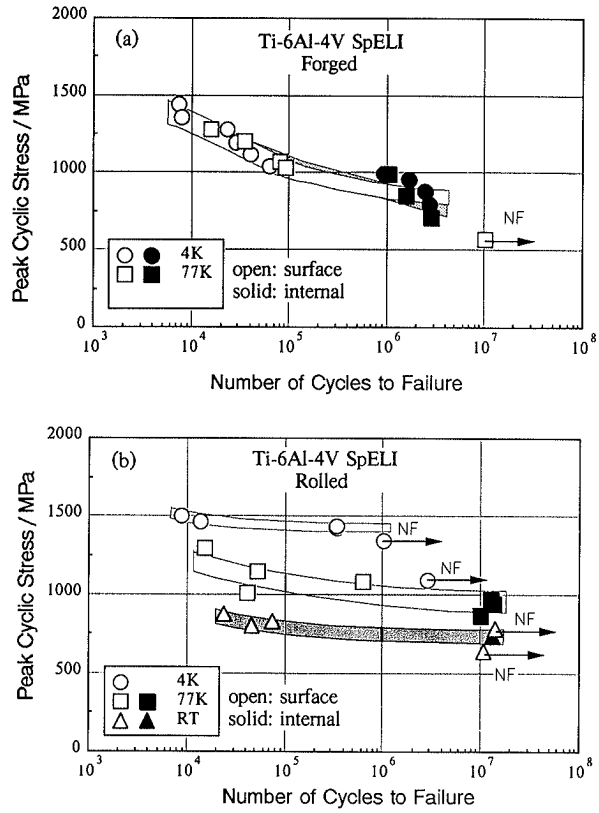

Fig. 10. S–N curves of Ti—6Al–4V SpELI alloys: (a) forged and (b) rolled.

elsewhere.[16]

3.4.1. Effect of Test Temperature

Temperature decrease produced an increase in strength, and generally it is said that the fatigue strength is proportional to the tensile strength. Hence a simple analogy leads to a speculation that the fatigue strength is increased at lower temperature. It is obviously true for the rolled materials irrespective of the oxygen level; the S–N curves shift to higher stress level at lower temperature and they are almost parallel. In the forged materials, on the other hand, there is nearly no gap between the S–N curves at 77 and 4 K. The S–N curve at 293 K was obtained only for the Normal alloy. In the regime of shorter fatigue lives, some gap in the S–N curves is observed between 293 and 77 or 4 K, however the gap becomes narrower as the number of cycles to failure increases and the S–N curves are supposed to overlap at around 5 million cycles.

In **Fig. 12**, one million cycles fatigue strength (MFS) is plotted as a function of test temperature. As far as the MFS is concerned, the MFS increases with a decrease in temperature and the rolled material is superior to the forged material at all the temperatures. Especially at 4 K, the difference in the MFS between two materials is distinctly large.

3.4.2. The Effect of Strength Level

Ratio of yield strength to tensile strength was higher than 95% at all the temperatures for three alloys. Therefore, the interrelation between strength and MFS is described in terms of yield strength *vs.* MFS as in **Fig. 13**, since yield strength is one of the most important

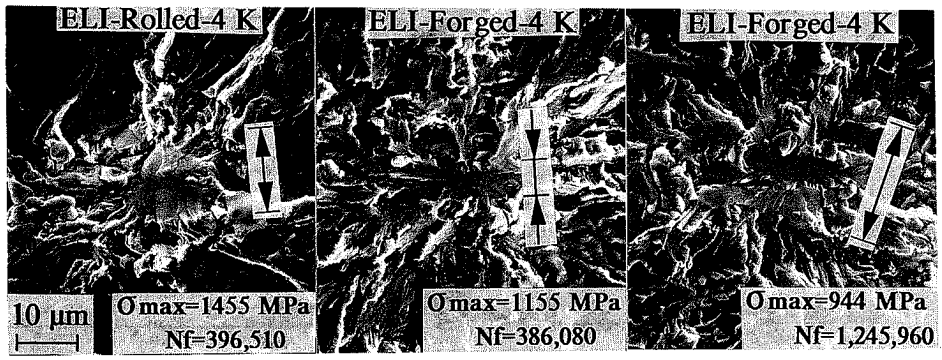

Fig. 11. SEM photographs of "Internal" fatigue crack initiation site for ELI alloy at 4 K.

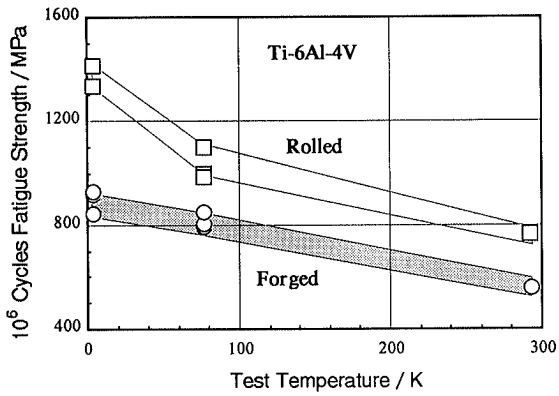

Fig. 12. One million cycles fatigue strength as a function of test temperature in the forged and the rolled materials.

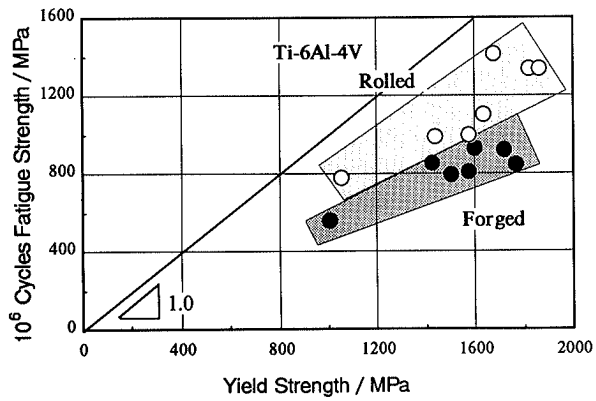

Fig. 13. Relationship between yield strength and one million cycles fatigue strength in the Ti–6Al–4V alloys.

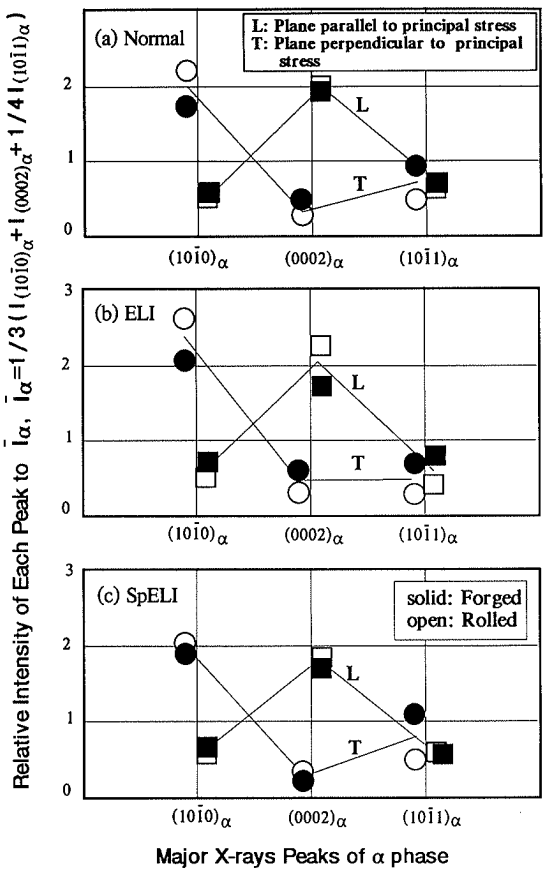

Fig. 14. X-rays relative intensities of major peaks of α phase.

measures in the selection of candidate materials. Anyway almost the same plotting was done when the tensile strength was taken as an *X*-axis.

As seen in Fig. 13, the plots form two separate groups when the processing is taken as a parameter. In other words, the MFS of the rolled material is higher than that of the forged material at a given yield strength. Roughly speaking, either in the rolled material or in the forged material, the MFS is proportional to the yield strength over the temperature range investigated. And the dependence of MFS on yield strength is less in the forged material than in the rolled material. This corresponds to the above-mentioned result in Fig. 12. Although more detailed comparison leads to a different conclusion that at 4 K the SpELI alloys having the lowest yield strength showed the higher MFS than other two alloys, this is considered to be no major concern except the fact that the SpELI alloy had the maximum MFS at 4 K.

3.4.3. Microstructural Factors and Fatigue Strength

Sommer *et al.* said that in the textured Ti–6Al–4V alloys the alternating stress parallel to c-axis introduced longer fatigue lives than that perpendicular to c-axis.[17] The alloys investigated here were also highly textured. Fig. 14 shows the simplified X-rays analysis of texture, namely X-rays intensities of three major peaks from prismatic plane, $(1010)_\alpha$, basal plane, $(0002)_\alpha$, and pyramidal plane, $(1011)_\alpha$ are shown in relative ratios to normalized total intensity,

$$I_\alpha (= 1/3(I_{(1010)_\alpha} + I_{(0002)_\alpha} + 1/4 I_{(1011)_\alpha})$$

This equation is based on the assumption that the ratio of the intensities is equal to 1 : 1 : 4 where the calculated

ratio is 23.2 : 25.0 : 100 for pure-Ti (Cu-Kα). Therefore the maximum of relative intensity, I/I_α, is 3.0 and the larger I/I_α shows the more preferred orientation. From **Fig. 14**, it is concluded that all the materials have the similarly textured microstructure in which the prismatic plane is perpendicular and the basal plane is parallel to the principal stress, that is, the *c*-axis perpendicular to the principal stress. And the texture is further accentuated in the rolled materials. Hence the difference in fatigue strength between the forged and the rolled materials can not be explained in terms of texture.

As explained earlier, a significant difference between the forged material and the rolled one was observed not in the primary α grain size itself, but in their morphology of primary α grains. The internal initiation site in the rolled material was globular and its size was several μm in diameter (Fig. 11(a)). In the forged material, the site was composed of elongated facets and the width of each facet was also several μm (Figs. 11(b) and 11(c)). The features of each facet correspond to those of primary α grain both in the rolled material and the forged one.

The comparison of Figs. 11 (a) and 11(b) demonstrates the internal cracking at lower stress level at 4 K in the forged material than in the rolled one with similar numbers of cycles for the ELI alloy. And in the forged one, the internal cracking occurs at further lower stress and the site size becomes larger (Fig. 11(c)). Some reported that finer primary α grain size produced higher fatigue strength.[18] In the forged material, the primary α grains in a colony are believed to be crystallographically aligned and act as a single path for dislocation moving.[19] In that case, the mean slip length becomes several times of primary α grain width in the forged material. In the rolled material, on the other hand, the mean slip length is considered to be of an order of single primary α grain size. Accordingly, the forged material has a longer slip length than the rolled material, which may introduce higher stress localization and easier crack initiation at the same applied stress and this leads to lower fatigue strength.

From these consideration, it is concluded that the significant difference in the fatigue strength was caused by the morphological change in their microstructure. In other words, the globular α grain microstructure produces a higher fatigue strength than the microstructure in which plate-like or elongated α grains of the same size form "colonies".

4. Summary

The effects of oxygen level and forming process on cryogenic mechanical properties were investigated for Ti–6Al–4V alloys. The oxygen level was nominally 0.05, 0.10, and 0.15 mass%, and each alloy was called Normal, ELI (abbreviating extra-low-interstitials), and SpELI (special ELI) alloy, respectively. The alloys were prepared both in the as-forged material and in the rolled material.

(1) Mean primary α grain size of the SpELI alloy was smallest. Although rolling did not always produce the finer α grain size, the process changed the morphology of α grains. Namely the globular grains were obtained in the rolled material in place of plate-like α grains forming "colony" in the forged one.

(2) Both yeild and tensile strengths increased with a decrease in temperature. The oxygen content dependence of yield strength surpassed the grain size dependence. The SpELI alloy had much better ductility at 4 K than other two.

(3) Fracture toughness was also highly dependent on the oxygen content. Reduction of oxygen suppressed the drop of low temperature fracture toughness. In the SpELI alloy, the fracture toughness was in the same level at all the temperatures.

(4) The fatigue strength of the rolled material was superior to that of the forged one especially at 4 K. At a given strength level, the former was higher than the latter over the temperature range investigated. This is believed to be ascribed to the difference in α grain morphology.

REFERENCES

1) K. Yoshida, H. Nakajima, K. Koizumi, M. Shimada, Y. Sanada, Y. Takahashi, E. Tada, H. Tsuji and S. Shimamoto: Austenitic Steels at Low Temperatures, Plenum Press, New York, (1983), 29.
2) K. Hirano: New Aspects of Non-magnetic Steels, ISIJ, Tokyo, (1990), 85.
3) K. Nagai and K. Ishikawa: *Tetsu-to-Hagané*, **75** (1989), 29.
4) K. Nagai, T. Ogata, T. Yuri, K. Ishikawa, T. Nishimura, T. Mizoguchi and Y. Ito: *Trans. Iron Steel Inst. Jpn.*, **27** (1987), 376.
5) R. L. Tobler: Cracks and Fracture, ASTM STP 601, ASTM, (1976), 346.
6) R. G. Broadwell and R. A. Wood: *Mat. Res. Standards*, **4** (1964), 549.
7) J. C. Christian, A. Hurlich, J. E. Chafey and J. F. Watson: *Proc. ASTM*, **63** (1963), 578.
8) J. C. Chesnutt and J. C. Williams: *Metall. Trans.*, **8A** (1977), 514.
9) ASM Metals Reference Book, ASM, Ohio, (1983), 385.
10) K. Nagai, T. Yuri, T. Ogata and K. Ishikawa: Cryogenic Materials '88, Vol. 2, ICMC, Boulder, (1988), 901.
11) T. Ogata, K. Ishikawa, K. Nagai, K. Hiraga, Y. Nakasone and T. Yuri: *Tetsu-to-Hagané*, **71** (1985), 236.
12) H. Suenaga, Y. Kohsaka and C. Ouchi: *Trans. Iron Steel Inst. Jpn.*, **26** (1986), 149.
13) K. Shibata: *Tetsu-to-Hagané*, **75** (1989), 213.
14) K. Nagai, K. Hiraga, T. Ogata and K. Ishikawa: *Trans. Jpn. Inst. Met.*, **26** (1985), 405.
15) T. Horiya, H. G. Suzuki and T. Kishi: *Tetsu-to-Hagané*, **75** (1989), 151.
16) O. Umezawa, K. Nagai and K. Ishikawa: *Tetsu-to-Hagané*, **76** (1990), 118.
17) A. Sommer, M. Creager, S. Fujishiro and D. Eylon: Titanium and Titanium Alloys, Scientific and Technological Aspects, ed. by J. C. Williams and A. F. Belov, Plenum Press, New York and London, (1982), 1863.
18) J. J. Lucas and P. P. Konieczny: *Metall. Trans.*, **2** (1971), 911.
19) R. Brown: Fracture and Fatigue, Elasto-Plasticity, Thin Sheet and Micromechanisms Problems, Proc. the 3rd Colloquium on Fracture, Ed. by J. C. Radon, Pergamon Press, London, (1980), 371.